Thermodynamic Interactions in Model Polyolefin Blends Obtained by Small-Angle Neutron Scattering

N. P. Balsara,*,† L. J. Fetters, N. Hadjichristidis,‡ and D. J. Lohse

Corporate Research Laboratories, Exxon Research and Engineering Company, Annandale, New Jersey 08801

C. C. Han

National Institute of Standards and Technology, Gaithersburg, Maryland 20899

W. W. Graessley* and R. Krishnamoorti

Department of Chemical Engineering, Princeton University, Princeton, New Jersey 08544

Received April 16, 1992; Revised Manuscript Received July 23, 1992

ABSTRACT: The dependence of Flory–Huggins interaction parameter χ on temperature, composition, and chain length was investigated for binary blends of amorphous model polyolefins, materials which are structurally analogous to copolymers of ethylene and butene-1. The components were prepared by saturating the double bonds of nearly monodisperse polybutadienes (78%, 88%, and 97% vinyl content) with H_2 and D_2, the latter to provide contrast for small-angle neutron scattering (SANS) experiments. Values of χ were extracted from SANS data in the single-phase region for two series of blends, H97/D88 and H88/D78, using the random-phase approximation and the Flory–Huggins expression for free energy of mixing. These values were found to be insensitive to chain length (one test only) and to the component volume fractions for $\phi = 0.25$, 0.50, and 0.75. Their temperature dependence (27–170 °C) obeys the form $\chi(T) = A/T + B$ with coefficients that connote upper critical solution behavior, yielding $T_c \sim 40$ °C for one blend series (H97A/D88) and $T_c \sim 60$ °C for the other (H88/D78). These estimates are consistent with SANS pattern changes and supplemental light scattering results that indicate two-phase morphologies at lower temperatures. The $\chi(T)$ coefficients for the two series are also consistent with the random copolymer equation, although the interaction parameter obtained for branch C_4–linear C_4 chain units is much larger than that found by Crist and co-workers for saturated polybutadienes with lower ethyl branch contents.

Introduction

Polymers are used in many applications as blends of two or more species. Mutual solubilities are usually limited, so multiphase materials are commonly obtained. Their properties depend crucially on the amount, composition, and morphological arrangement of the phases, as well as thickness and strength of the phase interfaces. All such features are related, directly or indirectly, to the thermodynamics of mixing in the melt state, yet remarkably little quantitative information is available even for systems of major commercial importance, such as polyolefins.

A natural starting point for the organization of data on two-component blends is the Flory–Huggins equation[1-3]

$$\frac{\Delta G_m}{k_B T} = \frac{\phi_1 \ln \phi_1}{v_1 N_1} + \frac{\phi_2 \ln \phi_2}{v_2 N_2} + \chi \frac{\phi_1 \phi_2}{v} \qquad (1)$$

where ΔG_m is the free energy of mixing per unit volume, k_B is Boltzmann's constant, T is the absolute temperature, ϕ_i, v_i, and N_i are volume fractions, volumes per monomeric unit, and polymerization indices of the components, v is an arbitrary reference volume, and χ is the interaction parameter. The first two terms represent the combinatorial entropy for random mixtures of chain molecules, while the last term provides for pairwise interactions between randomly mixed chain units. The latter may in principle consist of both enthalpic and entropic contributions, arising for example from changes with mixing in both local energetics and packing. Thus, to a first approximation

$$\chi = A/T + B \qquad (2)$$

where A and B specify the enthalpic and entropic parts of χ. Other forms of the temperature dependence have been considered[4] and may indeed be required, depending on the system and range of temperature.

Although χ should in principle be independent of ϕ, this is seldom found in practice. Possible reasons for this discrepancy are not difficult to identify. Some may arise from polydispersity of the individual components and from nonrandomness introduced by relatively strong specific interactions in some of the systems investigated.[3] Other have to do with various equation-of-state (EOS) effects,[5-9] related to differences in thermal expansion and compressibility of the components, and also with the mean-field character of the theory itself.[10-12] Indeed, χ is found to depend on ϕ even in the simplest possible test case of monodisperse isotopic mixtures,[13] where EOS differences are probably negligible. Likewise, χ should in principle be independent of N as well as other features of the large-scale chain architecture, but the evidence is still rather limited.[13,14]

Mixtures of structurally different species of saturated hydrocarbon polymers, such as polyolefins, represent a logical next step in microstructural complexity beyond the pioneering work of Bates and co-workers on isotopic mixtures.[15] Local packing effects, probably negligible in isotopic mixtures, may now become a significant factor because the chain units have different sizes and shapes. EOS effects should begin to play some role as well. However, because the polymers are aliphatic hydrocarbons (empirical formula CH_2 in all cases) the change in

† Current address: Department of Chemical Engineering, Polytechnic University, Brooklyn, NY 11201.
‡ Permanent address: Department of Chemistry, University of Athens, Athens 157 71, Greece.

0024-9297/92/2225-6137$03.00/0

Table I
Characterization Data from Dilute-Solution Light Scattering

	THF solution			cyclohexane solution		
sample	dn/dc[a]	$\bar{M}_w \times 10^{-4}$	$A_2 \times 10^4$ [b]	dn/dc[a]	$\bar{M}_w \times 10^{-4}$	$A_2 \times 10^4$ [b]
H78	0.083	7.08	7.4	0.061	7.32	10.6
H88	0.083	8.94	6.6	0.062	9.10	9.5
H97A	0.085	8.78	6.1	0.064	9.17	8.8
H97B	0.082	4.85	7.1	0.064	4.83	10.7

[a] Units are mL g^{-1}. [b] Units are mL mol g^{-2}.

intermolecular energy with mixing should be relatively small and purely dispersive in origin: permanent dipole effects and specific interactions, including the weak attraction between olefinic moieties that apparently stabilizes some polydiene mixtures,[16,17] are absent.

The work described here deals with the thermodynamics of model polyolefin blends, in which the components are structurally analogous to copolymers of ethylene and butene-1.[18] They are prepared by a two-step synthesis, anionic polymerization of butadiene followed by hydrogenation, to obtain saturated hydrocarbon polymers with different frequencies of ethyl branches (depending on the vinyl content of the polybutadiene precursor) distributed statistically along an otherwise linear hydrocarbon backbone:

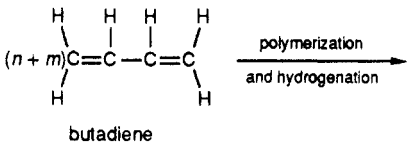

butadiene

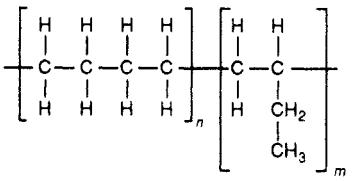

statistical copolymer

The samples are nearly monodisperse in molecular weight distribution and represent three chemical microstructures (32, 39, and 47 ethyl branches per 100 backbone carbons). Thermodynamic interactions in single-phase mixtures of these samples were obtained by small-angle neutron scattering (SANS). Light scattering measurements were also used in a few cases to locate phase boundaries. Crist and co-workers have investigated thermodynamics of mixing with hydrogenated polybutadienes of lower ethyl branch contents.[19,20]

The polymers are made in pairs by saturating the double bonds of the precursor polybutadienes with hydrogen in one case to make a fully hydrogenous version and with deuterium in another to make a partially deuterated version (fractional substitution f = [D]/([H] + [D]) ~ 0.35).[21] They should be identical in chemical microstructure and polymerization index and will be referred to here as matched pairs. The deuterated materials are necessary to provide contrast in the SANS experiments, but they also introduce the possibility of an isotopic contribution to the thermodynamics. Bates and coworkers[22] have studied the thermodynamic effects of isotopic substitution in mixtures of fully hydrogenous and fully deuterated samples of poly(ethylethylene), a polymer that is the structural equivalent of atactic polybutene-1 (50 ethyl branches per 100 backbone carbons) and also closely resembles the polymers in this study. For our materials we estimate an isotopic interaction parameter $\chi_{HD} \sim 1 \times 10^{-4}$ at 30 °C based on $\chi_{HD} \sim 9 \times 10^{-4}$ for the structurally similar poly(ethylethylene)[22] and an expected quadratic dependence on the fractional substitution f.[19,23] The effect of the interaction parameter on scattering behavior becomes significant when $\chi \gtrsim 1/N$ (see below), so with polymerization index $N \sim 10^3$, typical of the samples in this study, we can obtain values of the interaction parameter in the 10^{-3} range with reasonable accuracy. Thus, we expect the isotopic contribution to be small in our studies, although not necessarily negligible, compared with the effect of differences in chemical microstructure. We assess its magnitude more directly, however, from SANS measurements on the matched pair mixtures, where the isotopic interactions should dominate.

We use these materials to determine the composition and temperature dependence of χ for two series of blends with chemically different components for which the critical temperature T_c lies in our temperature window, 27–170 °C. We also present a preliminary investigation of the N dependence of χ and some new results, obtained from the matched pair experiments, on chain dimensions in the melt state.

Experimental Section

Polymer Synthesis and Characterization. Four samples of high vinyl polybutadiene—78, 88, 97A, and 97B—were prepared by anionic polymerization of butadiene in cyclohexane at ~0 °C. Vacuum-line conditions were used,[24] the initiator was *n*-butyllithium, and the terminating agent was degassed methanol. Promoters were employed to achieve the desired level of 1,2 (vinyl) additions—1,2-dipiperidinoethane (DIPIP) for the two samples with 97% 1,2 content (47 ethyl branches per 100 backbone carbons), tetramethylethylenediamine (TMEDA) for the sample with 88% 1,2 content (40 ethyl branches per 100 backbone carbons), and tetrahydrofuran (THF) for the sample with 78% 1,2 content (32 ethyl branches per 100 backbone carbons). Aliquots of these samples were dissolved in cyclohexane (CHN) and reacted with either H_2 or D_2 under pressure at 70 °C in the presence of a $Pd/CaCO_3$ catalyst.[25] This step was repeated when necessary until olefinic unsaturation was no longer detectable by proton NMR (<0.5% residual unsaturation). The resulting eight saturated polymers, four fully hydrogenous—H78, H88, H97A, H97B—and four partially labeled with deuterium—D78, D88, D97A, D97B—were separated from the residual catalyst by solution filtration (0.22-μm Anotop filters), then precipitated with an acetone/methanol mixture, and dried under vacuum.

Molecular weights were determined for the fully hydrogenous samples by light scattering (Chromatix KMX-6). Scattering intensity at small angles was measured for a series of dilute solutions in both CHN (distilled from CaH_2) and THF (distilled from Na). These results and the values of dn/dc in each solvent (Chromatix KMX-16) were then used[26] to obtain the values of $\bar{M}_w$ and the second virial coefficient A_2 listed in Table I.[27] The number of monomeric units per chain N was obtained by dividing $\bar{M}_w$ by the monomeric molecular weight for fully hydrogenous samples, m_0 = 56.11. The values of N in Table I, used in all subsequent calculations, are averages of the values obtained independently in CHN and THF.

Values of $\bar{M}_w/\bar{M}_n$ for all samples, including the parent polybutadienes, were estimated by size-exclusion chromatography in THF (Waters 150-C). The system was calibrated with both polystyrene and hydrogenated polyisoprene standards. The results were not corrected for axial dispersion. All distributions were narrow ($\bar{M}_w/\bar{M}_n = 1.06 \pm 0.01$), and the SEC traces for each parent polybutadiene, its fully hydrogenous derivative, and its partially deuterated derivative were superposable, confirming that no change in large-scale architecture had occurred during the saturation step. The same values of N were thus assumed to apply for both versions (fully hydrogenous and partially deuterated) in each matched pair. The results are given in Table II.

Table II
Molecular Characteristics of Hydrogenous and Partially Deuterated Polymers

sample	N	content of ethylethylene units[a]	T_G (°C)[b]	density (g mL^{-1}, at 23 °C)	n_D[c]
H78	1290	78	−45	0.8630	0
D78	1290	78		0.9002	2.37
H88	1610	88	−34	0.8642	0
D88	1610	88		0.9108	2.96
H97A	1600	97	−22	0.8658	0
D97A	1600	97		0.9098	2.79
H97B	865	97	−25	0.8651	0
D97B	865	97		0.9074	2.69

[a] Mol % of 1,2 units in precursor polybutadiene. [b] Glass transition temperature, obtained as the midpoint of the DSC transition for a heating rate of 10 °C/min. [c] Average number of deuterium atoms per C_4 unit, calculated from densities according to eq 3.

Density was determined at 23 °C with a density gradient column (ethylene glycol/methanol). Values obtained for the fully hydrogenous samples agreed well with densities reported elsewhere.[18] The results were used to calculate n_D, the average number of deuterium atoms per C_4 repeat unit in the partially deuterated samples:

$$n_D = 55.77\left(\frac{\rho_D - \rho_H}{\rho_H}\right)/\left(1 + 6.97\frac{\rho_D}{\rho_H}\beta\right) \quad (3)$$

where ρ_D and ρ_H are the densities for the partially deuterated and fully hydrogenous versions of the matched pair, and β is the fractional reduction in molar volume for full replacement of hydrogen by deuterium. Reported values of β for hydrocarbon polymers range from 0.002 to 0.004.[15] We have used $\beta = 0.002$ to obtain the values of n_D in Table II, but the adjustment in any case is small and comparable to the errors introduced by uncertainty in the density measurements (±0.0003), with n_D increased by ~1.5% for $\beta = 0$ and decreased by the same amount for $\beta = 0.004$. The values of n_D are larger than 2.0, indicating some H–D exchange occurs as well as saturation. Density was also routinely measured for the blends. The assumption of no volume change on mixing was confirmed in all cases within the precision of the density determinations.

The mol % of 1,2 additions was determined by proton NMR measurements on the parent polybutadienes[28] and by carbon-13 NMR measurements on their hydrogenated derivatives.[29] The results, which agree by the two methods within experimental error (±0.5–1.0%), are given in Table II. The carbon-13 NMR spectra were also used to investigate the local 1,2–1,4 sequencing along the chain. The results were cast in terms of reactivity ratio products, r_1r_2, as outlined by Hsieh and Randall.[29] The values $r_1r_2 = 0.73$ for H78 and $r_1r_2 = 0.66$ for H88, suggest an essentially random sequencing with perhaps a slight tendency toward alternation. Reliable values of r_1r_2 could not be obtained for H97A and H97B owing to their low level of 1,4 units. Stereospecificity of the 1,2 incorporations was not investigated, but earlier work on similar systems[30] suggests an essentially atactic configuration.

All samples are amorphous according to differential scanning calorimetry (Seiko, Model SSC5200H). Their glass transition temperatures are given in Table II.

Small-Angle Neutron Scattering. Blends were prepared by dissolving the components in cyclohexane, recovering either by evaporation or by precipitation with an acetone/methanol mixture, and then drying to constant weight in a vacuum oven at 60 °C. Samples for the scattering experiments (~0.23 g) were loaded between quartz disks, separated by an aluminum spacer (16-mm i.d., 1 mm thick), and mounted in brass cell holders.

The SANS measurements were performed on the 8-m beam line at the Cold Neutron Research Facility, National Institute of Standards and Technology (NIST).[31] Neutrons with wavelength $\lambda = 9.0$ Å ($\Delta\lambda/\lambda = 0.25$) were used. Scattering intensities were measured with a 64 cm × 64 cm area detector at a sample-to-detector distance of 3.6 m, providing a usable span of scattering vector magnitudes, $q = (4\pi/\lambda)\sin(\theta/2)$, in the range $0.8 \times 10^{-2} \lesssim q$ (Å^{-1}) $\lesssim 7.5 \times 10^{-2}$. A total of at least 10^6 detector counts was typically obtained, requiring counting times of 20–60 min per experiment. Measurements were made at temperatures of 27, 52, 84, 123, and 170 °C, and in that order, for most of the experiments. Measurements were sometimes also made in descending order when a phase transition occurred in the experimental range.

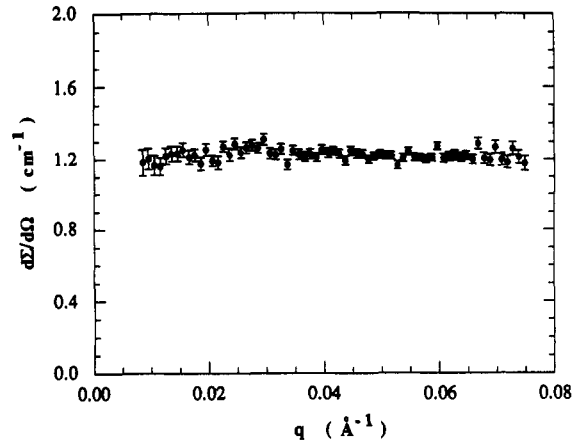

Figure 1. Scattering intensity for the fully hydrogenous polymer H97B at 27 °C. The error bars represent the uncertainties due to counting statistics.

The scattering data were corrected for background, empty cell scattering, and pixel-by-pixel detector sensitivity, the latter established from the incoherent scattering of a water sample. Sample transmissions were routinely determined at 27, 84, and 170 °C, although measurements at 52 and 123 °C were occasionally made to check the interpolations. The results were consistent with a recent study of the transmission coefficient and its temperature dependence;[32] corrections for multiple scattering[33] and for the effect of wavelength spread $\Delta\lambda/\lambda$ were found to be negligible. The correspondence between absolute scattering intensity $(d\Sigma/\Delta\Omega)_{total}$ and the detector counting rate was obtained from the scattering of a silica gel secondary standard provided by the Reactor Division at NIST. Comparison of size-exclusion chromatograms before and after the experiments showed no evidence of sample degradation.

All scattering patterns were azimuthally symmetric, so circularly averaged data were used in the analysis. The incoherent scattering intensity was assumed to scale with the concentration of hydrogen atoms in the sample and was determined from the scattering at 27, 84, and 170 °C for a fully hydrogenous sample, H97B. The result at 27 °C is shown in Figure 1. The scattering profile is flat for the range $1.0 \times 10^{-2} < q$ (Å^{-1}) $< 7.1 \times 10^{-2}$, with an average $(d\Sigma/d\Omega)_{total}$ of 1.22 cm^{-1}. The incoherent scattering for the blends was calculated with this value, the density of 0.863 for H97B at 27 °C, and the densities (ρ_H, ρ_D), volume fractions (ϕ_H, ϕ_D), and n_D of the blend components. Assuming no volume change on mixing and that all the incoherent scattering arises from the protons

$$\left(\frac{d\Sigma}{d\Omega}\right)_{inc} = \frac{1.22}{0.863}\left[\phi_H\rho_H + \phi_D\rho_D\left(\frac{8 - n_D}{8}\right)\left(\frac{56.11}{56.11 + n_D}\right)\right] \text{ cm}^{-1} \quad (4)$$

Values were calculated at other temperatures using eq 4 and the thermal expansion coefficient for poly(ethylethylene),[34] $\alpha = -d\ln\rho/dT = 6.0 \times 10^{-4}$ (°C)$^{-1}$, for all components. The measured values for H97B at 84 and 170 °C (1.21 and 1.19 cm^{-1}, respectively) agree with this formula.

The incoherent background was subtracted from the total scattering intensity to obtain the coherent contribution $(d\Sigma/d\Omega)_{coh}$. This was then converted to the static structure factor of the blend using the monomeric scattering contrast

$$S(q) = \left(\frac{d\Sigma(q)}{d\Omega}\right)_{coh}/\left(\frac{b_H}{v_H} - \frac{b_D}{v_D}\right)^2 \text{ cm}^3 \quad (5)$$

in which v_H and v_D are the volumes per C_4 unit for the component polymers at the temperature of the experiments, and b_H and b_D

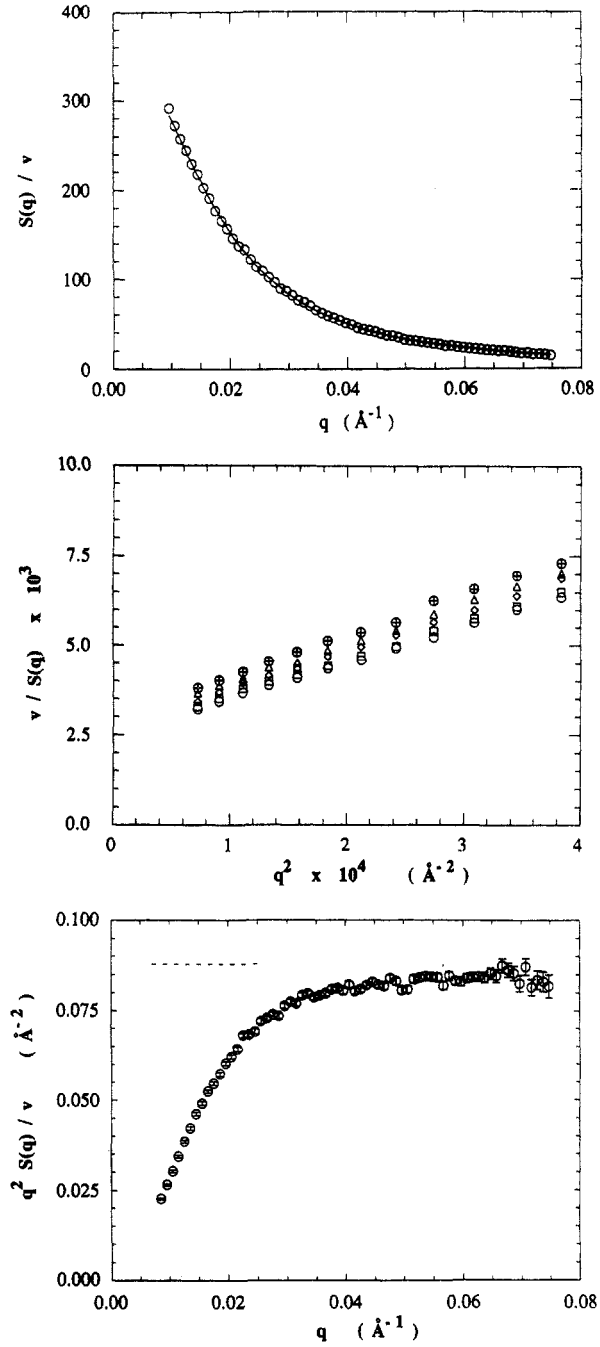

Figure 2. (a) Structure factor for the matched pair mixture H97A/D97A (ϕ = 0.50) at 27 °C. The solid line shows the full range fit of eq 11 to the data, with l and χ_{HD} as adjustable parameters. (b) Ornstein–Zernike plots for matched pair mixtures H97A/D97A (ϕ = 0.50) at several temperatures. Results in the low q range ($0.92 \times 10^{-2} \le q \le 1.98 \times 10^{-2}$ Å^{-1}) are shown for 27 °C (○), 52 °C (□), 84 °C (◇), 123 °C (△), and 170 °C (⊕). (c) Kratky plot for the matched pair mixture H97A/D97A (ϕ = 0.50) at 27 °C. The dashed line represents the Kratky plateau calculated from the fall range fit.

are the coherent scattering lengths per C_4 unit. The latter were calculated from the coherent scattering lengths for H, D, and C atoms[35] and the known atomic compositions of the C_4 units.

Analysis of SANS Data

The scattering data were analyzed within the general framework of the random-phase approximation (RPA), which provides a relationship[36] for the structure factor of a two-component, single-phase mixture obeying the Flory–Huggins theory. Although strictly speaking the components in our case are statistical copolymers, we treat them as homopolymers for purposes of analysis. Thus, from RPA and eq 1

$$\frac{1}{S(q)} = \frac{1}{v_1\phi_1 N_1 P_1(q)} + \frac{1}{v_2\phi_2 N_2 P_2(q)} - \frac{2\chi}{v} \tag{6}$$

where $P_1(q)$ and $P_2(q)$ are the normalized ($P_i(0) = 1$) form factors (partial structure factors) of the component polymers. For the reference volume we used the geometric average

$$v = (v_1 v_2)^{1/2} \tag{7}$$

For the form factors we use the Debye formula for monodisperse random-coil polymers:

$$P(u) = \frac{2}{u^2}[\exp(-u) - 1 + u] \tag{8}$$

$$u = (qR_G)^2 \tag{9}$$

where R_G is the radius of gyration. The radius and number of mers per molecule are related by

$$R_G^2 = l^2 N/6 \tag{10}$$

where l is the statistical segment length of the polymer. In the more general case, if the interaction parameter varies with blend composition, then χ in eq 6 is replaced by

$$-\frac{1}{2}\frac{\partial^2}{\partial\phi^2}[\phi(1-\phi)\chi(\phi)]$$

where ϕ can be either ϕ_1 or ϕ_2.

Equations 6–10 provide the basis for extracting values of l and χ_{HD} from the scattering data for matched pair mixtures and χ from the scattering data of chemically different polymers. A brief analysis of experimental errors is given in Appendix A.

Matched Pair Mixtures. Here the components differ only in isotopic substitution, and we assume $N_1 = N_2 \equiv N$ and $P_1(q) = P_2(q) \equiv P(q)$. Also, the volumes per C_4 unit are practically the same, so we use $v_1 = v_2 \equiv v$. Equation 6 thus reduces to

$$\frac{v}{S(q)} = \frac{1}{\phi_H\phi_D N P(q)} - 2\chi_{HD} \tag{11}$$

where ϕ_H and ϕ_D are volume fractions of the hydrogenous and partially deuterated members of the pair and χ_{HD} is the isotopic interaction parameter. Equal volume mixtures ($\phi_H = \phi_D = 0.5$) were used, except in one supplementary experiment as noted below.

The matched pair data were analyzed in several ways. Values of l and χ_{HD} were obtained by a nonlinear regression fit over the full q range. They were also obtained with the low q data alone from the initial slope and intercept of an Ornstein–Zernike plot, $v/S(q)$ vs q^2. From eqs 8–11

$$\frac{v}{S(q)} = \frac{v}{S(0)} + \frac{l^2}{18\phi_H\phi_D}q^2 + O(q^4) \quad (qR_G \ll 1) \tag{12}$$

where

$$\frac{v}{S(0)} = \frac{1}{\phi_H\phi_D N} - 2\chi_{HD} \tag{13}$$

Values of l were also obtained with the intermediate q data alone from the plateau of a Kratky plot, $q^2S(q)$ vs q.

Table III
Statistical Segment Lengths from Matched Pair Experiments

	l (Å)				
sample	27 °C	52 °C	84 °C	123 °C	170 °C
H78/D78	5.9_9	6.0_2	6.0_8	6.1_7	6.2_5
H88/D88	5.9_1	5.9_5	5.9_6	5.9_8	6.0_6
H97A/D97A	5.8_4	$5.8/_6$	6.0_3	6.1_5	6.2_9
	5.7_5[a]				6.2_0[a]
	5.7_8[b]				
H97B/D97B	5.2_1	5.2_2	5.2_6	5.3_0	5.3_3

[a] Repeat experiment with a new blend of the components. [b] ϕ_D = 0.05. All other results obtained with $\phi_H = \phi_D = 0.50$.

Table IV
Isotopic Interaction Parameters Obtained from Matched Pair Experiments

	$(\chi_{HD})_{apparent} \times 10^4$ [a]				
sample	27 °C	52 °C	84 °C	123 °C	170 °C
H78/D78	0.3_6	0.2_9	-0.6_5	-0.9_2	-1.1_8
H88/D88	1.5_8	1.1_8	0.3_0	-0.8_0	-1.5_7
H97A/D97A	-1.4_6	-1.9_0	-2.4_5	-2.9_8	-3.7_4
	-0.8_9[b]				-3.2_8[b]
H97B/D97B	0.5_6	0.2_8	-0.1_0	-0.5_9	-0.9_9

[a] Designated as apparent values because they are, for the most part, small and comparable to the errors in evaluating the absolute structure factors (see Appendix A). All results obtained with $\phi_H = \phi_D = 0.5$. [b] Repeat experiment with a new blend of the components.

From eqs 8–11

$$\frac{q^2S(q)}{v} = \frac{12\phi_H\phi_D}{l^2} \quad (l \ll q^{-1} \ll R_G) \tag{14}$$

Figure 2a shows the fit obtained over the full q range for the 97A matched pair at 27 °C. Ornstein–Zernike plots of the low q data at all temperatures is shown in Figure 2b, and a Kratky plot at 27 °C is shown in Figure 2c. The values of l from the full range fit and from the Kratky plateau were always in good agreement, but those from the low q data alone (eq 13) were usually somewhat larger. The latter seem less reliable, however, because qR_G is never smaller than about 0.8 in our experiments. The full range fits, on the other hand, are heavily weighted by the low q data since the counting errors are smallest there, and the intermediate q Kratky plateaus are experimentally well-defined (Figure 2c is typical), as found by similar studies in this range.[37] Thus the agreement in l obtained by these two procedures is reassuring and provides significant confirmation of the RPA framework for data analysis. The values of l obtained by full range fits are listed in Table III.

The values obtained for χ_{HD} by full range fits are listed in Table IV. Except for 97A, the deviations from the ideal intercepts ($4/N$ at $\phi_H = \phi_D = 0.5$ in eq 13) are less than 10%. Thus, the true magnitudes of χ_{HD} are almost certainly masked by errors in absolute calibration, molecular weight, and contrast factor (Appendix A). On the other hand, such errors should be independent of temperature, yet $(\chi_{HD})_{apparent}$ for each matched pair varies systematically with the temperature, corresponding to decreases in $S(0)/v$ of 10–30% from 27 to 170 °C, depending on the sample. Also, the rather large negative values obtained for the 97A pair are puzzling, but aside from those the magnitudes of $(\chi_{HD})_{apparent}$ are small and in the 10^{-4} range estimated above. We have not used those values in analyzing the results for blends of chemically different polymers.

Blends of Chemically Different Polymers. Some blends were phase-separated at room temperature but then passed into the one-phase region at an elevated temperature. Despite the similarity in component refractive indices, this change was even evident by visual inspection. The two-phase blends, as mounted between quartz disks for SANS, were clear when viewed by transmitted light but showed a fine, pebble-grained appearance in reflection. The pebbled pattern disappeared at elevated temperatures but then reappeared slowly (hours to days) after cooling again to room temperature. This behavior, also seen in phase-separated isotopic mixtures,[23] was monitored more quantitatively by light scattering and used to define the transition temperature (see Appendix B).

The existence of two phases was also detectable in the SANS data from the presence of anomalously strong forward scattering and a correspondingly diminished scattering at higher q. The scattering pattern also depended on the thermal history of the sample, presumably through its relationship to the extent of "ripening" of a two-phase morphology. The pattern also evolved slowly with time when the temperature was increased, sometimes requiring several hours to stabilize at the new temperature.

Such time- and history-dependent effects were absent in the single-phase blends. The SANS pattern equilibrated quickly when the temperature was changed, and the differences were consistent with single-phase RPA and the matched pair data. Thus, from eq 6, the initial slope of an Ornstein–Zernike plot should depend only on the segment lengths and monomeric volumes of the components:

$$\frac{1}{S(q)} = \frac{1}{S(0)} + \left[\frac{l_1^2}{v_1\phi_1} + \frac{l_2^2}{v_2\phi_2}\right]\frac{q^2}{18} + O(q^4)$$

The slopes should therefore be rather insensitive to temperature and predictable from the matched pair results. The same should apply to the Kratky plateau, which eq 6 gives as

$$q^2S(q) = 12\left[\frac{l_1^2}{v_1\phi_1} + \frac{l_2^2}{v_2\phi_2}\right]^{-1} \quad (l \ll q^{-1} \ll R_G) \tag{15}$$

When good agreement was found in both magnitude and temperature insensitivity for the low q slope and intermediate q plateau, we assumed the blend was single phase. We took increased slopes and diminished plateaus to be the signatures of a two-phase blend.

Ornstein–Zernike and Kratky plots are shown for the H88/D78 ($\phi = 0.5$) blend at five temperatures in Figure 3a,b. Initial slopes and plateaus predicted from matched pair data are also shown. The slope and plateau at 84, 123, and 170 °C agree reasonably well with the predictions, but those at 27 and 52 °C are progressively different, indicating that the blend becomes single phase somewhere between 52 and 84 °C. Light scattering (see Appendix B) showed that the transition actually takes place between 65 and 70 °C. The same comparisons are shown for the H97A/D88 blend (ϕ(H97A) = 0.75) in Figure 4a,b. Slopes and plateaus in this case are consistent with predictions at all temperatures, indicating a single phase over the entire range. The distinction between one and two phases became particularly difficult near the critical composition. Thus, for the H97A/D88 blend at $\phi = 0.50$ the slopes and plateaus seemed consistent with RPA at all temperatures, but the Ornstein–Zernike intercept was negative at 27 °C, indicating two phases at that temperature.

Values of χ were extracted from the data on blends in the single-phase region by a variety of procedures. In one we assumed that the form factors of the components, obtained in the matched pair experiments, would be

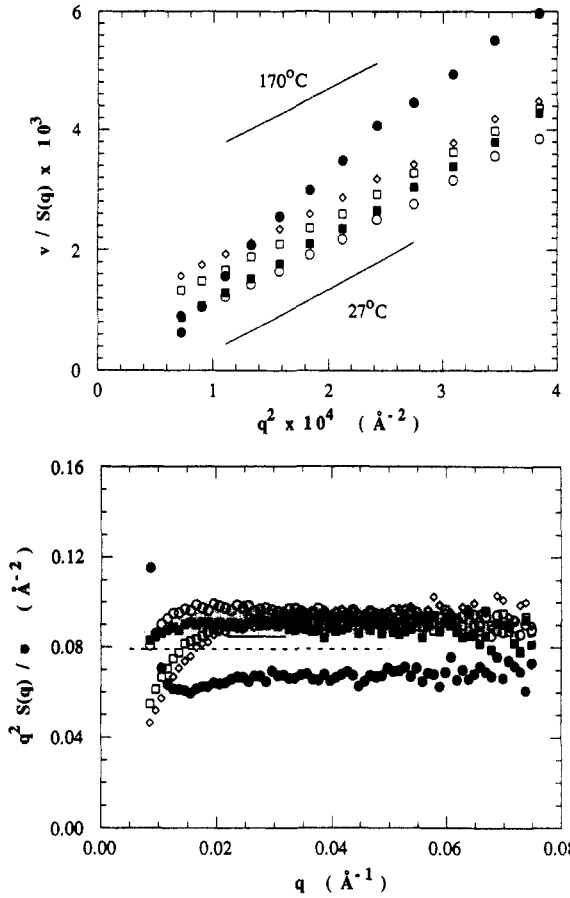

Figure 3. (a) Ornstein–Zernike plots for the H88/D78 ($\phi = 0.50$) blend at several temperatures. The solid line represents the initial slope ($q \to 0$) predicted with the matched pair data. The slopes at 84 (○), 123 (□), and 170 °C (◇) are in reasonable agreement with that prediction and with each other, while those at 27 (●) and 52 °C (■) are progressively larger. (b) Kratky plots for the H88/D78 ($\phi = 0.50$) blend at several temperatures. The solid and dashed lines represent the Kratky plateaus predicted with the matched pair data at 27 and 170 °C, respectively. The plateaus at 84 (○), 123 (□), and 170 °C (◇) are in reasonable agreement with that prediction and with each other, while those at 27 (●) and 52 °C (■) are progressively lower.

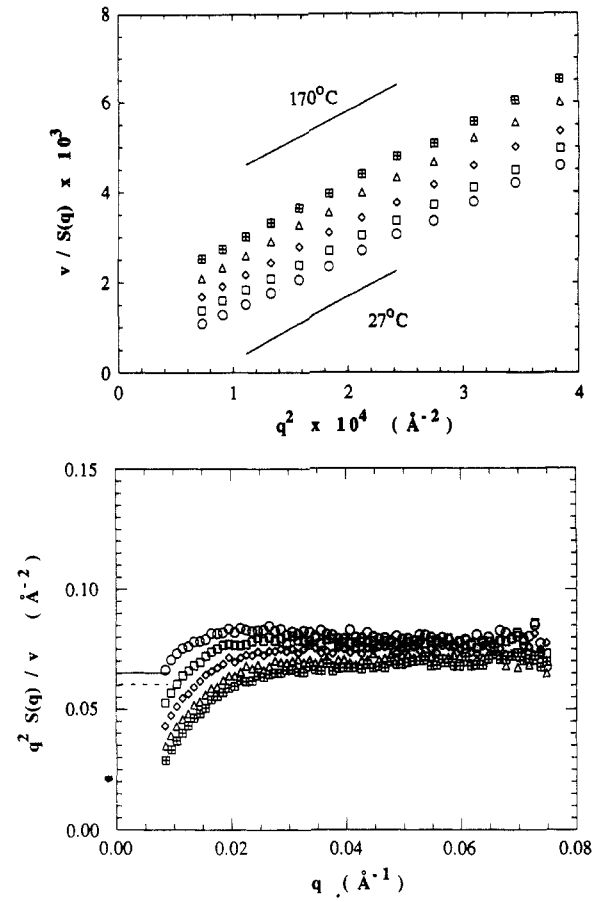

Figure 4. (a) Ornstein–Zernike plots for the H97A/D88 (ϕ(H97A) = 0.75) blend at several temperatures. The solid line represents the slope predicted with the matched pair data. (b) Kratky plots for the H97A/D88 (ϕ(H97A) = 0.75) blend at several temperatures. The solid and dashed lines represent the plateaus predicted with the matched pair data at 27 and 170 °C, respectively.

essentially unchanged in the blends. Structure factors for ideal mixing were calculated from the matched pair data:

$$\left(\frac{1}{S(q)}\right)_{\text{ideal}} = \frac{1}{v_1\phi_1 N_1 P_1(q)} + \frac{1}{v_2\phi_2 N_2 P_2(q)} \qquad (16)$$

The result is compared with the experimental $S(q)$ for the H97A/D88 blend ($\phi = 0.50$, 52 °C) in Figure 5a. The differences at each q were then calculated point by point to obtain an excess function, defined as

$$E(q) = \frac{v}{2}\left[\left(\frac{1}{S(q)}\right)_{\text{ideal}} - \frac{1}{S(q)}\right] \qquad (17)$$

If RPA and Flory–Huggins were strictly valid, $E(q)$ would be independent of q and equal to χ for the blend. In practice, $E(q)$ was found to depend weakly on q, as shown by the example in Figure 5b, but the value of $q = 0$ can in any case be obtained by a relatively easy extrapolation. We used that intercept

$$\chi = E(0) \qquad (18)$$

to define the interaction parameters listed in Tables V and VI.

As an alternative, we used the more direct procedure of extrapolating Ornstein–Zernike plots for the blend to obtain $v/S(0)$ and then calculating χ from the $q = 0$ limit of eq 6:

$$\chi = \frac{v}{2}\left[\frac{1}{v_1\phi_1 N_1} + \frac{1}{v_2\phi_2 N_2} - \frac{1}{S(0)}\right] \qquad (19)$$

These values were found to differ only negligibly from those obtained by the first procedure. We also applied nonlinear regression and the RPA scattering expression (eq 6) to the data. The fitting parameters in this case were χ and $\kappa = l/l_0$, where l_0 is the segment length of each component, as obtained in the matched pair experiments. Again, the values of χ agreed with those obtained by the $E(q)$ extrapolation. The values of κ were always close to unity (see Figure 6), but the average for all blends was slightly smaller ($\kappa_{av} = 0.96$), suggesting a mild contraction of chain dimensions in the blends, where the interactions are stronger than those in the matched pair experiments. Such behavior has been observed before[38] and is consistent at least qualitatively with the findings in recent Monte Carlo simulations.[39] It appears in a different guise as the mild q dependence found in $E(q)$ (Figure 5b).

Results and Discussion

97/88 Blends. The interaction parameters obtained for blends of samples H97A and D88 at $\phi = 0.25$, 0.50, and 0.75 of H97A are listed in Table V. The values of χ at each temperature are similar, although there may be some slight trend toward higher values for $\phi = 0.25$ and $\phi = 0.75$ at the lower temperatures. Within the experimental errors, however, the values are independent of composition over this range. The temperature dependence of χ, plotted

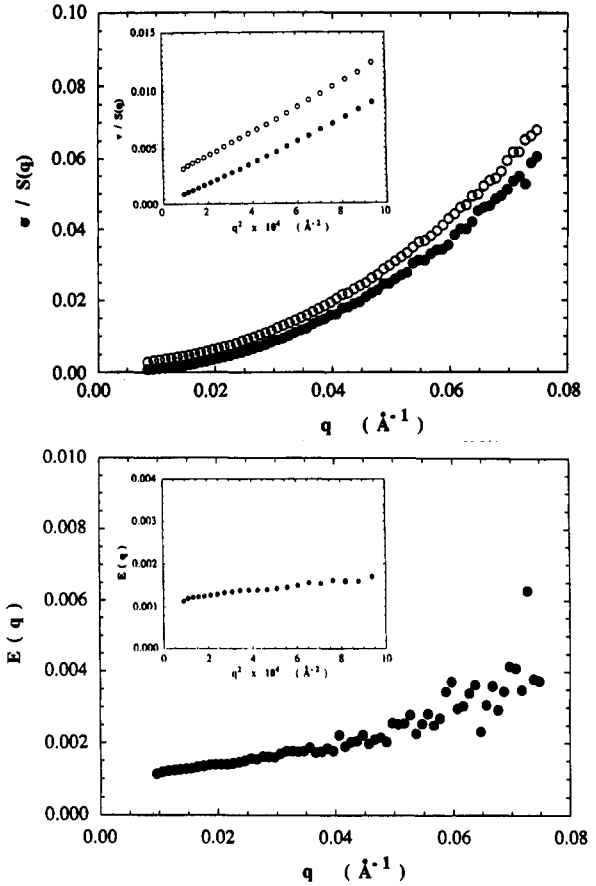

Figure 5. (a) Comparison of the reciprocal structure factor for the H97A/D88 (ϕ = 0.50) blend at 52 °C with that obtained for ideal mixing from the matched pair data. The inset shows the corresponding Ornstein–Zernike plots at low q for the observed (●) and ideal (○) behavior. (b) Excess function $E(q)$ for the H97A/D88 (ϕ = 0.50) blend at 52 °C. The inset shows the corresponding Ornstein–Zernike plot at low q.

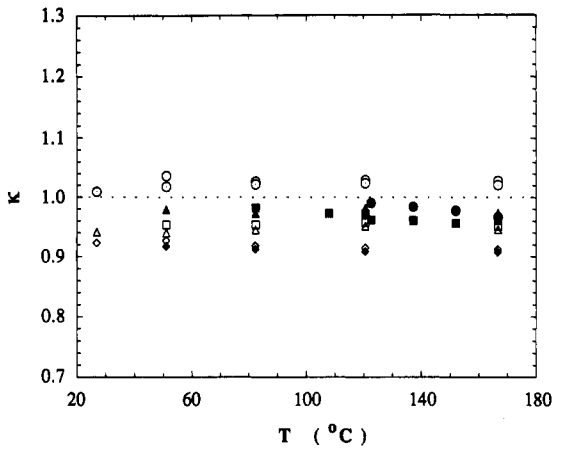

Figure 6. Ratio of statistical segment lengths in blends relative to matched pair values. The open symbols correspond to H97/D88 blends and the filled symbols to H88/D78 blends.

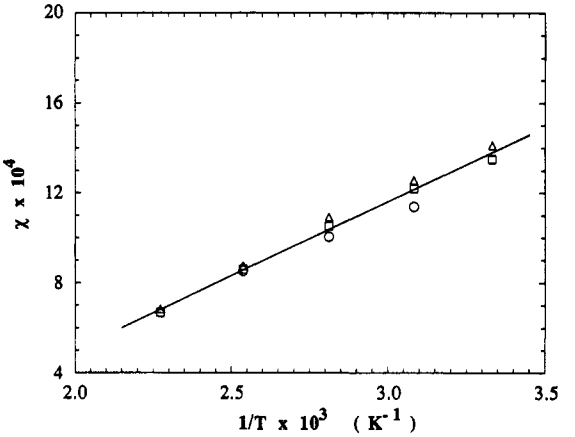

Figure 7. Temperature dependence of interaction parameters obtained for the H97A/D88 blend series. Values are shown for ϕ(H97A) = 0.25 (□), 0.50 (○), and 0.75 (△).

according to eq 2, is shown in Figure 7. The results for $0.25 \leq \phi \leq 0.75$ are reasonably well described by

$$\chi = 0.66/T - 8.2 \times 10^{-4} \tag{20}$$

For binary blends that conform to Flory–Huggins, the critical composition and value of χ at the critical temperature are given by

$$(\phi_2)_c = \frac{(v_1N_1)^{1/2}}{(v_1N_1)^{1/2} + (v_2N_2)^{1/2}} \tag{21}$$

$$\chi_c = \frac{v}{2}\left[\frac{1}{(v_1N_1)^{1/2}} + \frac{1}{(v_2N_2)^{1/2}}\right]^2 \tag{22}$$

For the H97A/D88 blends (N_1 = 1600, N_2 = 1610), these give ϕ_c = 0.50 and $\chi_c = 1.25 \times 10^{-3}$, which corresponds to T_c = 47 °C from eq 20. If $\chi(T)$ at ϕ = 0.50 alone is used (52 °C and above), a critical temperature of 35 °C is obtained. This difference is well within the errors of the experiment, and both results are consistent with our inference from the SANS patterns that two phases are present for ϕ = 0.50 at 27 °C but only one phase at 52 °C and above. Further experiments are planned at compositions below ϕ = 0.25 and above ϕ = 0.75, where Bates et al.[13] observe an upturn in χ for isotopic mixtures. For $0.25 \leq \phi \leq 0.75$ at least the results here indicate rather good agreement with the Flory–Huggins theory and a composition-independent χ. The equilibrium phase diagram and the spinodal curve for H97A/D88 mixtures

Table V
Interaction Parameters Obtained for H97A/D88 and H97B/D88 Blends

	$\chi \times 10^4$				
ϕ	27 °C	52 °C	84 °C	123 °C	170 °C
0.25 (H97A)	13.5	12.2	10.5	8.6	6.7
0.50 (H97A)	(2-phase)	11.4	10.0	8.5	6.7
0.75 (H97A)	14.1	12.6	10.9	8.7	6.8
0.50 (H97B)	12.3	11.0	9.4	7.6	5.3

Table VI
Interaction Parameters Obtained for H88/D78 Blends

	$\chi \times 10^4$				
ϕ	27 °C	52 °C	84 °C	123 °C	170 °C
0.25 (H88)	(2-phase)	13.7	11.7	10.1	8.5
0.50 (H88)	(2-phase)	(2-phase)	12.4	10.2	8.5
0.75 (H88)	(2-phase)	15.4	12.9	10.7	8.6

calculated with eq 20 and the Flory–Huggins theory are shown in Figure 8.

The interaction parameters for H97B/D88 and H97A/D88 can be compared in Table V. The value of N for the 97 component differs by nearly a factor of 2, but all other conditions are the same. The enthalpic part of χ is virtually the same for H97A/D88 and H97B/D88, but the entropic part for H97B/D88 is slightly smaller, corresponding to a reduction of the total χ by ~5% at 52 °C and ~20% at 170 °C. The critical temperature for H97B/D88 blends, based on its own $\chi(T)$ data, is −30 °C, in reasonable agreement with the value of −40 °C obtained with $\chi(T)$ for the H97A/D88 blends (eq 20). We cannot rule out a

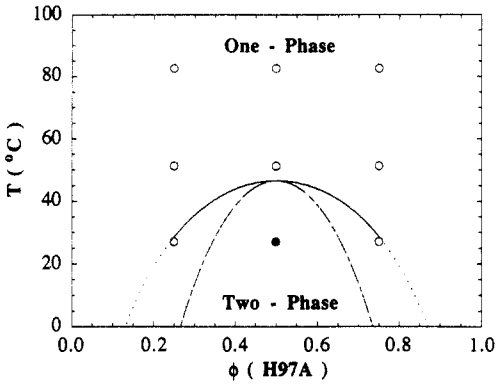

Figure 8. Calculated phase diagram and spinodal for H97A/D88 blends. The coexistence (solid) and spinodal (long dash-short dash) curves were obtained with the Flory–Huggins theory and $\chi(T)$ as given by eq 20. The circles indicate SANS measurements, showing one-phase (○) and two-phase (●) patterns.

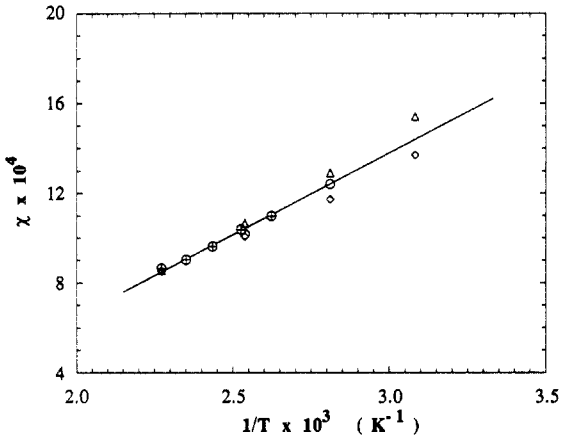

Figure 9. Temperature dependence of interaction parameters obtained for the H88/D78 blends. The symbols correspond with ϕ(H88) = 0.25 (◇), 0.50 (○), and 0.75 (△) by successive heating and 0.50 by successive cooling (⊕).

dependence of χ on N, but it is certainly small. Again the behavior is consistent with Flory–Huggins theory.

88/78 Blends. The values of $\chi(T)$ obtained by SANS for blends of H88 and D78 at three compositions (ϕ = 0.25, 0.50, and 0.75) are listed in Table VI. The situation is very similar to that found in the 97/88 blends, although the range is now slightly smaller because the two-phase region occupies a larger portion of our temperature–composition window. Thus, at ϕ = 0.50 the blend is two-phase at 27 and 52 °C but single-phase at 84 °C and above (see Figure 3a,b), while at both ϕ = 0.25 and ϕ = 0.75 the blend is two-phase at 27 °C but single-phase at 52 °C and above. Agreement in χ for the three compositions is good at 84 °C and above, although there may be a slight trend toward increasing values with increasing ϕ (H88). However, the largest difference between values at ϕ = 0.25 and ϕ = 0.75 is ~10% at 52 °C, which is still within the error bounds. The temperature dependence of χ for all compositions are plotted in Figure 9, including data obtained by successive cooling as well as successive heating. All results are reasonably well described by

$$\chi = 0.74/T - 8.4 \times 10^{-4} \quad (23)$$

The critical composition according to Flory–Huggins (eq 21) is ϕ_c = 0.47 (H88), and the value of χ at the critical temperature (eq 22) is $\chi_c = 1.39 \times 10^{-3}$. From eq 23, the latter corresponds to T_c = 65 °C. Using the data at ϕ = 0.5 alone, we obtain T_c = 58 °C. From light scattering (Appendix B) the boundary between the one-phase and two-phase regions at ϕ = 0.50 lies between 65 and 70 °C. All these results are consistent within the error bounds. Like the 97/88 blends, the 88/78 blends from ϕ = 0.25 to ϕ = 0.75 behave in reasonable accord with the Flory–Huggins theory.

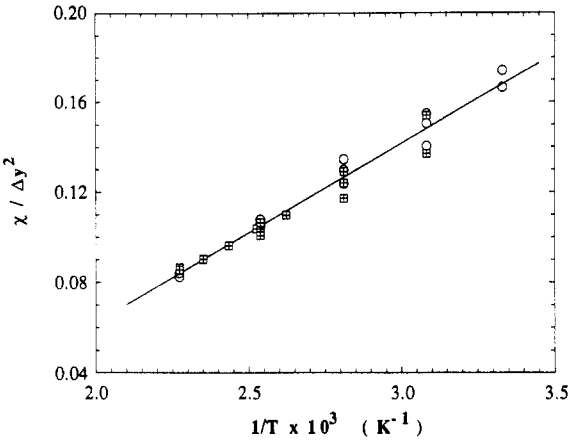

Figure 10. Test of interaction parameters for agreement with random copolymer theory. Data are shown for both H97A/D88 blends (○) and H88/D78 blends (⊞).

Intercomparisons. According to random copolymer theory,[40-42] and in the absence of isotopic contributions, the interaction parameters for mixtures of copolymers are related in a simple way to χ_h for mixtures of the homopolymer species and the difference $\Delta y = y_1 - y_2$ in mole fractions of the component mers in the copolymers:

$$\chi = \chi_h(\Delta y)^2 \quad (24)$$

All data for the H97A/D88 blends (Δy = 0.97 − 0.88 = 0.09) and the H88/D78 blends (Δy = 0.88 − 0.78 = 0.10) are plotted as $\chi(T)/(\Delta y)^2$ vs $1/T$ in Figure 10. A single line accommodates all the results reasonably well:

$$\chi = [81/T - 0.101](\Delta y)^2 \quad (25)$$

The term in brackets represents χ_h for homopolymers of the linear C_4 units (polyethylene) and the branched C_4 units (atactic polybutene-1). From eq 25, χ_h = 0.085 at 150 °C, a value which is considerably larger than χ_h = 0.014 obtained at 150 °C by Nicholson, Finerman, and Crist[19] from SANS measurements and χ_h = 0.022 obtained by Rhee and Crist[20] from T_c determinations, in both cases with blends of saturated polybutadienes with lower ethyl branch contents.

Some experiments were conducted with blends of H97B and D78 to test more fully the generalization embodied by eq 25. The difference in chemical microstructure is now larger, Δy = 0.97 − 0.78 = 0.19. Hence, the expected values of χ are much larger, and the predicted T_c much higher, than in the H97/D88 and H88/D78 blends. A blend far from the critical composition was prepared, ϕ(H97B) = 0.90, and SANS measurements were performed at temperatures up to 210 °C. The results are shown as Kratky plots in Figure 11 along with the single-phase plateau calculated from matched pair data. The blend is strongly two-phase at lower temperatures, but the plateau begins to grow above 123 °C and is not far from the single-phase prediction at 210 °C. From eq 25 and Flory–Huggins theory the transition to single phase for an H97B/D78 blend of this composition is predicted to be slightly above 200 °C, demonstrating a reasonable consistency with the copolymer equation and data obtained for the H97/D88 and H88/D78 blends.

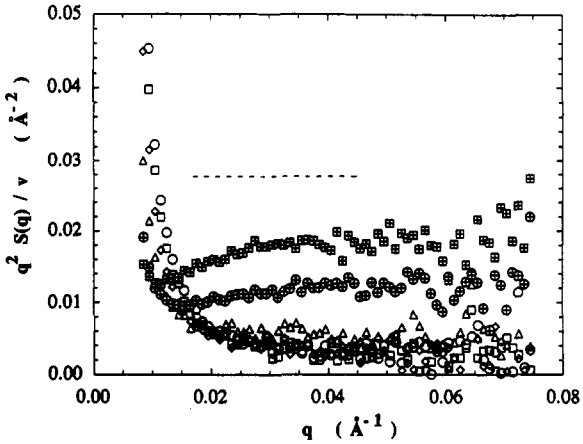

Figure 11. Kratky plots for the H97B/D78 (ϕ(H97B) = 0.1) blend at several temperatures. The solid line represents the plateau predicted from matched pair data at 170 °C. Data at 123 °C and below (○, △, □, ◇) indicate a strongly phase-separated morphology, but the behavior at 170 (⊕) and 210 °C (⊞) suggests an approach to the single-phase region not far above 210 °C.

Concluding Remarks

Thermodynamic interactions between saturated hydrocarbon polymers with different chemical microstructures have been measured in the single-phase melt state by SANS. The results obtained thus far for two series of blends, H97/D88 and H88/D78, conform to a simple and reasonably coherent pattern of behavior. Within each series $\chi(T)$ is insensitive to blend composition over the mid-range ($0.25 \leq \phi \leq 0.75$) and also to component molecular weight (the H97A/D88 and H97B/D88 comparison). The $\chi(T)$ values for the two series are consistent with the equation for random copolymers, eq 24, and in one case at least (the H97B/D78 experiment) with predictions based on that equation. A thorough examination of the random-phase approximation was conducted; the structure factors of the blends and the form factors of the pure components were measured in independent SANS experiments. We find that RPA works fairly well, although perhaps with some slight contraction of chain dimensions in the blends relative to matched pair values. There is also good agreement between light scattering measurements and predictions based on $\chi(T)$ in the location of phase boundaries.

Despite this seeming consistency, however, there remain some features that require further attention. For example, the matched pair experiments yielded different statistical segment lengths for samples 97A and 97B, l = 5.8 and 5.2 Å at 27 °C, respectively (Table III), despite their supposedly identical chemical microstructures. Bates et al.[22] found l = 4.9 Å at 26 °C from SANS measurements on a 50/50 mixture of hydrogenous and perdeuterated samples for the structurally similar poly(ethylethylene), and Hattam et al.[34] recently reported l = 5.3 Å for poly(ethylethylene) for Θ-solvent measurements near room temperature. The 97A matched pair experiment was repeated with fresh samples using ϕ_D = 0.50 and ϕ_D = 0.05, but in both cases l = 5.8 Å again was obtained (Table III). Moreover, the values for samples 88 and 78, l = 5.9 and 6.0 Å at 27 °C (Table III), are also larger than expected from interpolations of Θ-solvent data for other hydrogenated polybutadienes to those microstructures. Crist et al.[43] have also found "elevated" values of l from SANS measurements on hydrogenated polybutadienes having somewhat lower ethyl branch frequencies. These differences lie well beyond the estimated error bounds, and adjustments for differences in polydispersity are simply too small to account for them. It seems unlikely that they arise from some systematic error in our procedures because we find good agreement in l between our matched pair SANS data (unpublished) and Θ-solvent measurements for a variety of other model polyolefins (hydrogenated samples of 1,4-polyisoprene,[44] 1,4-poly(1,3-dimethylbutadiene),[44] and 1,4-poly(2-ethylbutadiene)[34]. Our results for hydrogenated 1,4-polyisoprene also agree with SANS values obtained at much lower labeled chain concentrations.[45] We believe our differences from Θ-solvent values are real for the hydrogenated polybutadiene materials but have been unable to account for them.

The effect of deuterium substitution on thermodynamic behavior also remains a matter of some concern. The fact that only partial substitution is used, and that $(\chi_{HD})_{apparent}$ from the matched pair experiments is relatively small (Table IV), would seem to offer assurance that interactions in the blends are dictated primarily by the differences in chemical microstructure. However, we have found that experiments in which the deuterium labeling is reversed can give rather different results. Thus, for example, the critical temperatures for D88/H78 blends and H88/D78 blends differ by nearly 70 °C. We have since found other examples in which large differences result from reversing the deuterium labels. Crist has also observed large effects due to label reversal.[43] The quantitative interpretation of results in terms of the interactions when both components are hydrogenous must obviously await a more detailed understanding of this phenomenon.

Acknowledgment. Support by the National Science Foundation through a grant to Princeton University (DMR89-05187) is gratefully acknowledged by W.W.G. and R.K. We thank Frank Bates and Buckley Crist for their comments, suggestions, and generosity in sharing information prior to publication, Richard Register for his very useful criticisms of the analysis, Charles Glinka and John Barker for their advice and help with the SANS experiments, and Robert Butera for his many contributions in the initial stages of the work.

Appendix A. Estimates of Errors

The main sources of error in evaluating the segment length l and interaction parameter χ are as follows: (a) SANS calibration, for converting count rates to absolute intensity units; (b) contrast factor, for converting coherent intensity to structure factor; (c) component molecular weights, for subtracting out the ideal mixing contribution to the structure factor. Counting statistics must also be considered in all experiments, including transmission measurements, background corrections, and incoherent intensity evaluations. Their effects are generally smaller, however, except in the determination of l from the Kratky plateau, but even there the statistics are adequate (see Figures 2b, 3b, and 4b, for example). More imponderable are errors associated with our extensive use of RPA to interpret the matched pair results and to assist the q = 0 extrapolations for the blends.

The translation from azimuthally averaged intensity expressed as count rates to the reported values of χ proceeds as follows:

$$\frac{v}{S(0)} = \frac{I_s(0)}{I(0) - I_{inc}}\left[\left(\frac{d\Sigma_s(0)}{d\Omega}\right)^{-1}\right] \times \left(\frac{\kappa}{\kappa_s}\right)\left(\frac{d}{d_s}\right)\left[\frac{(a_H - a_D)^2}{v} n_D^2\right] \quad \text{(A1)}$$

Table VII
Error Ranges for the 88 (ϕ = 0.50) Matched Pair Results

temp (°C)	$\chi \times 10^4$	l (Å)
27	$1.5_8 \pm 1.3_1$	$5.9_1 \pm 0.2_1$
52	$1.1_8 \pm 1.3_4$	$5.9_5 \pm 0.2_2$
84	$0.3_0 \pm 1.4_0$	$5.9_6 \pm 0.2_2$
123	$-0.8_0 \pm 1.4_8$	$5.9_8 \pm 0.2_2$
170	$-1.5_7 \pm 1.5_3$	$6.0_6 \pm 0.2_3$

where

$$\frac{\upsilon}{S(0)} = \frac{1}{\phi_1 N_1} + \frac{1}{\phi_2 N_2} - 2\chi \qquad \text{(A2)}$$

and where $I(0)$, $I_s(0)$, and I_{inc} refer to count rates for the sample, the silica gel standard, and the incoherent contribution; κ/κ_s and d/d_s are ratios of sample to standard transmission coefficients and thicknesses, respectively; $[(a_H - a_D)^2/\upsilon]n_D^2$ is the scattering contrast (here we use $\upsilon_1 = \upsilon_2 = \upsilon$ for simplicity); and $d\Sigma_s(0)/d\Omega$ is the intensity calibration for the standard. Among the various factors that govern $\upsilon/S(0)$ we assign the uncertainties

$\frac{I_s(0)}{I(0) - I_{inc}}$ ±2%, based mainly on comparisons of different extrapolation techniques

$\frac{d\Sigma S(0)}{d\Omega}$ ±5%, based on the considerations in refs 33, 46, and 47

$\left(\frac{\kappa}{\kappa_s}\right)\left(\frac{d}{d_s}\right)$ ±1%, based on reproducibility and errors in the thickness measurement

n_D^2 ±4%, based mainly on ±0.0003 for the density measurements

which lead to overall $\upsilon/S(0)$ uncertainties of ~7%. Combining this with eq A2 and with an estimated ±5% uncertainty in polymer molecular weight, we obtain

$$\chi = \frac{1}{2}\left[\left(\frac{1}{\phi_1 N_1} + \frac{1}{\phi_2 N_2}\right) \pm 5\% - \frac{\upsilon}{S(0)} \pm 7\%\right] \qquad \text{(A3)}$$

Note that eq A2 can be written more generally as

$$\frac{\upsilon}{S(0)} = 2[\chi(T_s) - \chi(T)] \qquad \text{(A4)}$$

where T_s is the spinodal temperature for the mixture. Thus, the values assigned to χ at temperatures far removed from T_s (the matched pair mixtures) are subject to all the errors embodied in eq A3, while those closer to T_s (the blends, and especially near the critical composition) will become mainly sensitive to the errors in the molecular weight alone.

The spans of scale factors in eq A3 were applied in full q range fits of the H88/D88 (ϕ = 0.5) matched pair data to obtain the uncertainties in l and χ_{HD} shown in Table VII. It is clear from those results that the true magnitudes of χ_{HD} are unobtainable from our data, while the uncertainty in l is 3–4%. The same spans were applied to the H97A/D88 (ϕ = 0.50) blend data, with results for the interaction parameters shown in Figure 12. The absolute uncertainty in χ is practically independent of temperature, ranging from $\pm 0.7 \times 10^{-4}$ at 52 °C to $\pm 1.0 \times 10^{-4}$ at 170 °C.

Appendix B. Light Scattering Study

The apparatus used in the light scattering experiments is sketched in Figure 13. The polymer blends are mounted as in the SANS experiments, i.e., between two quartz windows separated by a 1-mm-thick aluminum spacer. A beam of light from a 15-mW HeNe laser is directed through the sample, which is housed in an electrically-heated aluminum block. A CN 4700 Omega temperature controller is used to control the sample temperature. The scattered light in the angular range from 5° to 17° (corresponding to q values ranging from 1.3×10^{-4} to 4.5×10^{-4} Å^{-1}) is focused onto a photodetector, using the lens and the beam stop. The output of the detector is fed to a chart recorder.

The results obtained from a H88/D78 (ϕ = 0.5) blend are shown in Figure 14. The sample was first equilibrated at 100 °C, which is well above its phase transition temperature, and then quenched to various temperatures

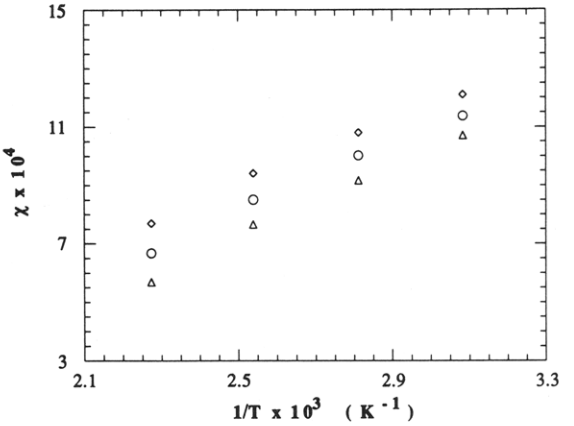

Figure 12. Influence of errors on interaction parameters for the H97A/D88 (ϕ = 0.50) blend. They represent the values as reported (○) and values obtained with the uncertainties specified in eq A3 (◇, △).

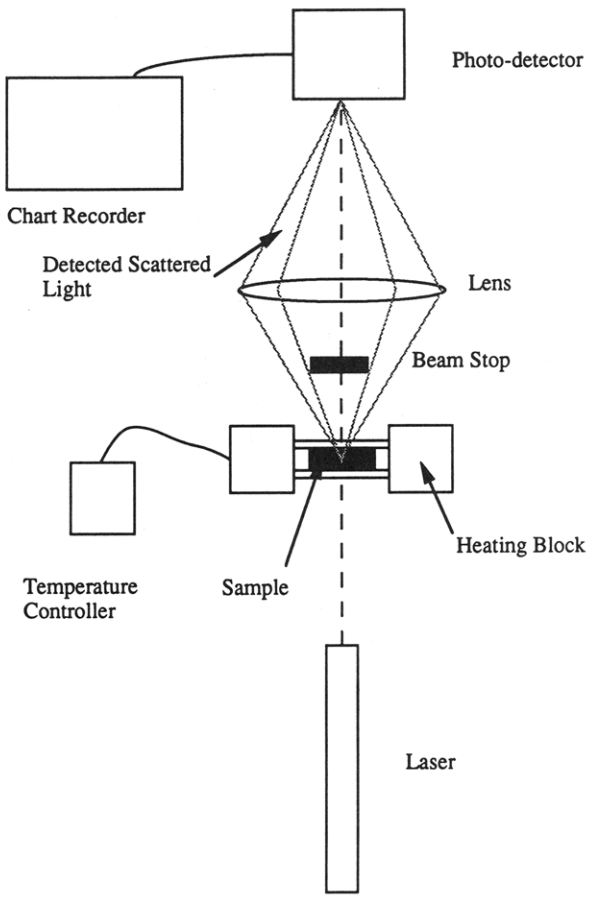

Figure 13. Diagram of the light scattering apparatus.

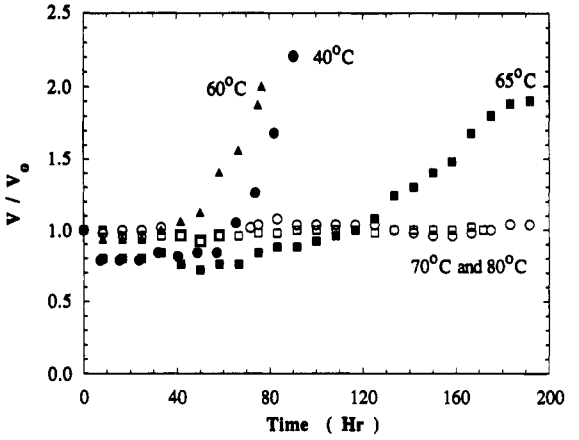

Figure 14. Normalized light scattering intensity for the H88/D78 (ϕ = 0.50) blend. Quenched from 100 °C. Quench temperatures are 40 (●), 60 (■), 65 (▲), 70 (○), and 80 °C (□).

(40, 60, 65, 70, and 80 °C). The time dependence of the photodetector voltage V, normalized by V_0, the reading at 100 °C, is plotted as a function of time since quenching. Temperature equilibration was reached in roughly 20 min.

The scattered intensity at 40 °C remained roughly constant for 60 h and then began to increase monotonically, as would be expected from a system undergoing phase separation. The scattering pattern was also visually observed by placing a screen in front of the lens. A spinodal ring was observed at times greater than 60 h, indicating two phases at this temperature. The sample was then reheated to 100 °C and quenched to 60 °C. The results obtained from this quench are similar to those obtained from the 40 °C quench. The increase in intensity is registered at shorter times, presumably due to increased molecular mobility at the higher temperature. An intensity growth was also observed at 65 °C, although more slowly in this case, probably because the supercooling is now very small. The scattered intensity obtained after quenching the sample to 80 °C was roughly constant for 150 h (about 1 week), and no spinodal ring was observed. The same result was obtained at 70 °C, in this case out to nearly 200 h. We thus conclude that the blend is still single-phase at 70 °C and that the phase boundary for this system lies between 65 and 70 °C.

References and Notes

(1) Huggins, M. L. *J. Chem. Phys.* **1941**, *9*, 440; *J. Phys. Chem.* **1942**, *46*, 151. Flory, P. J. *J. Chem. Phys.* **1941**, *9*, 660; *J. Chem. Phys.* **1942**, *10*, 51.
(2) Scott, R. L.; Magat, M. *J. Chem. Phys.* **1945**, *13*, 172.
(3) Olabisi, O.; Robeson, L. M.; Shaw, M. J. *Polymer–Polymer Miscibility*; Academic Press: New York, 1979.
(4) Koningsveld, R. *Adv. Colloid Interface Sci.* **1968**, *2*, 151.
(5) Flory, P. J. *J. Am. Chem. Soc.* **1965**, *87*, 1833.
(6) Sanchez, I. C.; Lacombe, R. H. *J. Phys. Chem.* **1976**, *80*, 2352 and 2568.
(7) Patterson, D.; Robard, A. *Macromolecules* **1978**, *11*, 690.
(8) Walsh, D. J.; Rostami, S. *Adv. Polym. Sci.* **1985**, *70*, 119.
(9) Dudowicz, J.; Freed, K. F. *Macromolecules* **1991**, *24*, 5112.
(10) Binder, K. *Colloid Polym. Sci.* **1988**, *266*, 871.
(11) Olvera de la Cruz, M.; Edwards, S. F.; Sanchez, I. C. *J. Chem. Phys.* **1988**, *89*, 1704.
(12) Schweizer, K. S.; Curro, J. G. *J. Chem. Phys.* **1989**, *91*, 5059.
(13) Bates, F. S.; Muthukumar, M.; Wignall, G. D.; Fetters, L. J. *J. Chem. Phys.* **1988**, *89*, 535.
(14) Han, C. C.; Bauer, B. J.; Clark, J. C.; Muroga, Y.; Matsushita, Y.; Odada, M.; Tran-cong, Q.; Chang, T.; Sanchez, I. C. *Polymer* **1988**, *29*, 2002.
(15) Bates, F. S. *J. Appl. Crystallogr.* **1988**, *21*, 681.
(16) Roland, C. M. *J. Polym. Sci., Part B: Polym. Phys.* **1988**, *26*, 839.
(17) Sakurai, S.; Hasegawa, H.; Hashimoto, T.; Hargis, I. G.; Aggarwal, S. L.; Han, C. C. *Macromolecules* **1990**, *23*, 451.
(18) Krigas, T. M.; Carella, J. M.; Struglinski, M. J.; Crist, B.; Graessley, W. W.; Schilling, F. C. *J. Polym. Sci., Polym. Phys. Ed.* **1985**, *23*, 509.
(19) Nicholson, J. C.; Finerman, T. M.; Crist, B. *Polymer* **1990**, *31*, 2287.
(20) Rhee, J.; Crist, B. *Macromolecules* **1991**, *24*, 5663.
(21) Tanzer, J. D.; Bartels, C. R.; Crist, B.; Graessley, W. W. *Macromolecules* **1984**, *17*, 2708.
(22) Bates, F. S.; Fetters, L. J.; Wignall, G. D. *Macromolecules* **1988**, *21*, 1086.
(23) Bates, F. S. Private communication.
(24) Morton, M.; Fetters, L. J. *Rubber Chem. Technol.* **1975**, *48*, 359.
(25) Rachapudy, H.; Smith, G. G.; Raju, V. R.; Graessley, W. W. *J. Polym. Sci., Polym. Phys. Ed.* **1979**, *17*, 1211.
(26) Fetters, L. J.; Hadjichristidis, N.; Lindner, J. S.; Mays, J. W.; Wilson, W. N. *Macromolecules* **1991**, *24*, 3127.
(27) Certain equipment and instruments or materials are identified in this paper in order to adequately specify the experimental details. Such identification does not imply recommendation by the National Institute of Standards and Technology, nor does it imply the materials are necessarily the best available for the purpose.
(28) Tanaka, Y.; Takeuchi, Y.; Kobayashi, M.; Tadakoro, H. *J. Polym. Sci., Polym. Phys. Ed.* **1971**, *9*, 43.
(29) Hsieh, E. T.; Randall, J. C. *Macromolecules* **1982**, *15*, 353.
(30) Xu, Z.; Hadjichristidis, N.; Carella, J.; Fetters, L. J. *Macromolecules* **1983**, *16*, 925.
(31) Glinka, C. J.; Rowe, J. M.; LaRock, J. G. *J. Appl. Crystallogr.* **1986**, *19*, 427.
(32) Coyne, L. D.; Wu, W. L. *Polym. Commun.* **1989**, *30*, 312.
(33) Wignall, G. D.; Bates, F. S. *J. Appl. Crystallogr.* **1987**, *20*, 28.
(34) Hattam, P.; Gauntlett, S.; Mays, J. W.; Hadjichristidis, N.; Young, R. N.; Fetters, L. J. *Macromolecules* **1991**, *24*, 6199.
(35) Bacon, G. E. *Neutron Diffraction*, 3rd ed.; Oxford University Press: London, 1975.
(36) de Gennes, P.-G. *Scaling Concepts in Polymer Physics*; Cornell University Press: Ithaca, NY, 1979.
(37) Crist, B.; Wignall, D. G. *J. Appl. Crystallogr.* **1988**, *21*, 701.
(38) Walsh, D. J.; Higgins, J. S.; Doupé, C. P.; McKeown, J. G. *Polymer* **1981**, *22*, 168.
(39) Sariban, A.; Binder, K. *Macromolecules* **1988**, *21*, 711.
(40) Scott, R. L. *J. Polym. Sci.* **1952**, *9*, 423.
(41) ten Brinke, G.; Karasz, F. E.; MacKnight, W. J. *Macromolecules* **1983**, *16*, 1827.
(42) Paul, D. R.; Barlow, J. W. *Polymer* **1984**, *25*, 487.
(43) Crist, B. Private communication.
(44) Mays, J. W.; Fetters, L. J. *Macromolecules* **1989**, *22*, 921.
(45) Zirkel, A.; Richter, D.; Pyckhout-Hintzen, W.; Fetters, L. J. *Macromolecules* **1992**, *25*, 954.
(46) Glinka, C.; Krueger, S. Memorandum to SANS users, Dec 29, 1986.
(47) Glinka, C. Private communication.